iScience

CellPress
OPEN ACCESS

Article

Experimental prognostic model integrating N6-methyladenosine-related programmed cell death genes in colorectal cancer

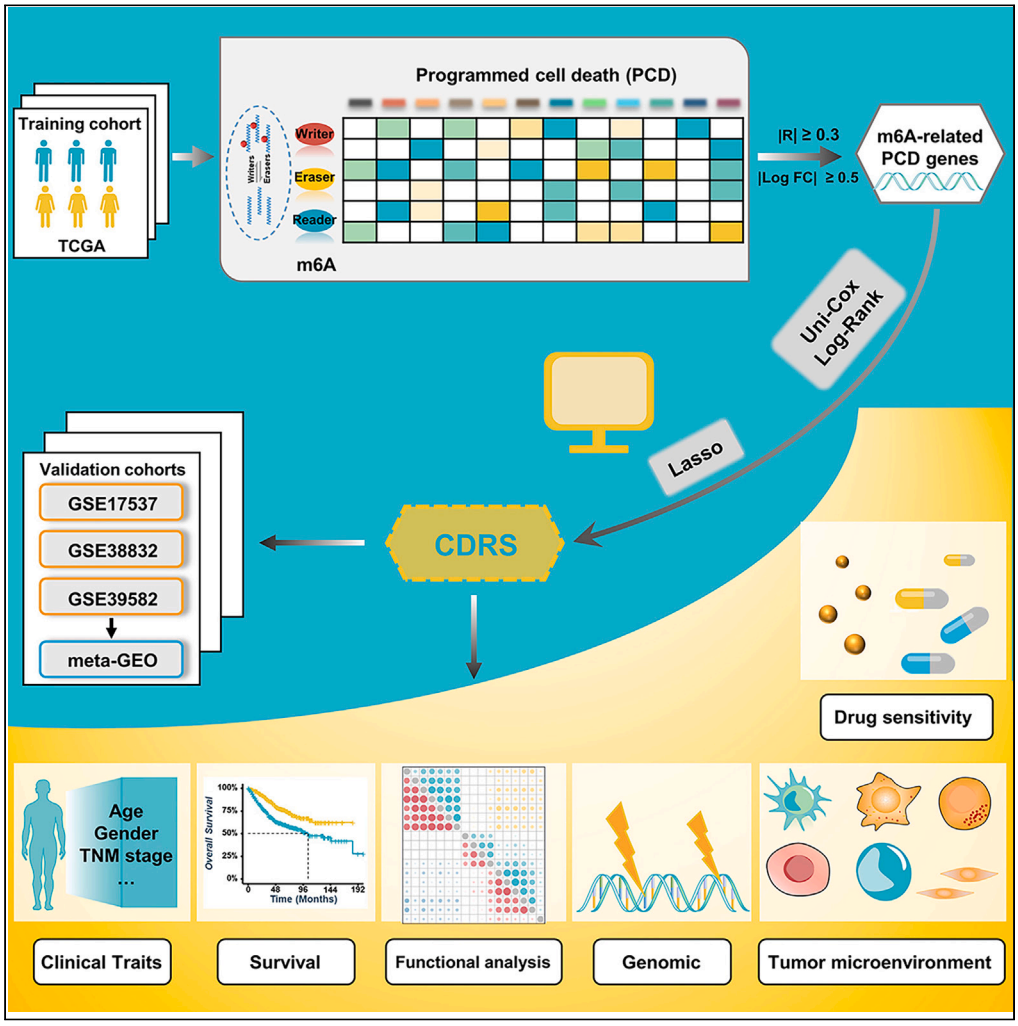

Qihui Wu, Xiaodan Fu, Xiaoyun He, Jiaxin Liu, Yimin Li, Chunlin Ou

yimin_li_0107@163.com (Y.L.)
ouchunlin@csu.edu.cn (C.O.)

Highlights

Identified a 10-gene signature for CRC prognosis

Explored biological pathways linked to CDRS and the relationship with TME

Experimental validation of CDRS genes in CRC cell lines and tissue samples

CDRS informs drug choices, aiding personalized treatment in patients with CRC

Wu et al., iScience 27, 108720
January 19, 2024
https://doi.org/10.1016/j.isci.2023.108720

iScience

CellPress
OPEN ACCESS

Article

Experimental prognostic model integrating N6-methyladenosine-related programmed cell death genes in colorectal cancer

Qihui Wu,[1,7] Xiaodan Fu,[2,7] Xiaoyun He,[3] Jiaxin Liu,[4] Yimin Li,[5,*] and Chunlin Ou[2,6,8,*]

SUMMARY

Colorectal cancer (CRC) intricacies, involving dysregulated cellular processes and programmed cell death (PCD), are explored in the context of N6-methyladenosine (m6A) RNA modification. Utilizing the TCGA-COADREAD/CRC cohort, 854 m6A-related PCD genes are identified, forming the basis for a robust 10-gene risk model (CDRS) established through LASSO Cox regression. qPCR experiments using CRC cell lines and fresh tissues was performed for validation. The CDRS served as an independent risk factor for CRC and showed significant associations with clinical features, molecular subtypes, and overall survival in multiple datasets. Moreover, CDRS surpasses other predictors, unveiling distinct genomic profiles, pathway activations, and associations with the tumor microenvironment. Notably, CDRS exhibits predictive potential for drug sensitivity, presenting a novel paradigm for CRC risk stratification and personalized treatment avenues.

INTRODUCTION

Colorectal cancer (CRC) ranks as the third most prevalent cancer worldwide, with almost 2 million cases diagnosed in 2020. It is also the second leading cause of cancer-related death, resulting in nearly 1 million annual fatalities, accounting for approximately one-tenth of all cancer cases and deaths.[1–4] Overall, CRC is the third most diagnosed cancer but the second deadliest.[5] Standard treatments for CRC include surgery, adjuvant or neoadjuvant chemotherapy and radiotherapy, as well as targeted therapy.[5] Despite advances in surgical and adjuvant therapies over the past few decades, survival for patients with advanced-stage CRC remains challenging, especially for those with distant metastases such as the liver or lung.[6] One major explanation for this is the lack of effective prognostic markers. Recently, increasing evidence suggests that gene expression profiling can be utilized to estimate the survival of patients with cancer.[7–12] Therefore, it is imperative to identify additional prognostic biomarkers that can stratify patients with CRC based on risk, enabling a more precise prediction of patient prognosis and even facilitating the development of personalized treatment plans, ultimately improving the survival rate of patients with CRC.

While both genetic and environmental factors are implicated in the development of CRC, recent studies have identified dysregulated RNA modifications, such as N6-methyladenosine (m6A), as important contributors to cancer progression and development.[13,14] m6A RNA modification, a reversible modification widely distributed in most RNA species, has been shown to participate in various aspects of RNA metabolism regulation, including transcription, processing, and stability.[15,16] The abundance and effects of m6A on RNA are determined by the dynamic interplay between its methyltransferase ("writers"), binding protein ("readers"), and demethylase ("erasers").[17] Additionally, m6A can be co-transcriptionally regulated through a variety of transcription factors.[18,19] Increasing evidence suggests that m6A plays a critical role in normal physiology as well as diseases, including cancer, and its dysregulation is associated with tumor microenvironment (TME) remodeling.[20–22] In CRC, abnormal m6A modification has been reported to be associated with tumor growth, metastasis, and poor prognosis.[23,24]

Programmed cell death (PCD) is a critical process that maintains tissue homeostasis by eliminating unnecessary or damaged cells.[25] PCD encompasses several major types, including apoptosis, necrosis, ferroptosis, pyroptosis, cuproptosis, parthanatos, alkaliptosis, oxeiptosis, netotic cell death, entotic cell death, lysosome-dependent cell death, autophagy-dependent cell death, and so forth.[26] For decades, PCD has been recognized as a fundamental process in both the development and metastasis of malignant tumors. Malignant tumor cells cannot progress further without overcoming various forms of cell death. Aberrant regulation of PCD genes has also been shown to contribute to the occurrence and progression of CRC.[27] otably, recent studies have indicated that m6A modification can regulate the expression of PCD genes,

[1]Department of Gynecology, Xiangya Hospital, Central South University, Changsha 410008, China
[2]Department of Pathology, Xiangya Hospital, Central South University, Changsha 410008, China
[3]Departments of Ultrasound Imaging, Xiangya Hospital, Central South University, Changsha 410008, China
[4]Department of Pathology, School of Basic Medical Sciences, Central South University, Changsha 410078, China
[5]Department of Pathology, Ruijin Hospital, Shanghai Jiaotong University School of Medicine, Shanghai 200025, China
[6]National Clinical Research Center for Geriatric Disorders, Xiangya Hospital, Changsha 410008, China
[7]These authors contributed equally
[8]Lead contact
*Correspondence: yimin_li_0107@163.com (Y.L.), ouchunlin@csu.edu.cn (C.O.)
https://doi.org/10.1016/j.isci.2023.108720

thereby playing a crucial role in the onset and progression of cancer.[13,28] However, the role of m6A RNA modification in regulating PCD during CRC development remains largely unexplored.

In this study, our aim was to investigate the role of m6A-related PCD genes in the management of CRC. We established a risk model based on m6A-related PCD genes using LASSO Cox regression analysis. This model identified 10 m6A-related PCD genes, which we subsequently validated through qPCR experiments using CRC cell lines and fresh tissues. The resulting cell death-related risk score (CDRS) was constructed based on these 10 genes and was found to be an independent risk factor for CRC. Notably, the CDRS exhibited superior accuracy in predicting prognosis compared to other clinical and molecular features. Furthermore, we unveiled a close relationship between CDRS and the tumor microenvironment (TME) and provided valuable insights for personalized chemotherapy drug selection. Our research has unveiled novel pathways for CRC risk stratification, holding the potential to guide personalized treatment and optimize the management of patients with CRC.

RESULTS

Identifying and validating N6-methyladenosine-associated programmed cell death genes in patients with colorectal cancer

To gain insight into the role of m6A-associated PCD in CRC, we initiated our investigation by analyzing the expression of m6A regulatory factors, which comprised 8 "writers," 13 "readers," and 2 "erasers," in both CRC and normal tissues. The results revealed that in CRC, 6 "writers" (CBLL1, METTL3, RBM15, RBM15B, VIRMA, ZC3H13) and 9 "readers" (ELAVL1, FMR1, HNRNPA2B1, IGF2BP1/2/3, LRPPRC, YTHDC1, YTHDF1) displayed upregulated expression (Figure S1A). To explore their prognostic significance in CRC, we conducted Cox regression analysis and Kaplan-Meier survival analysis. The results identified ELAVL1, FMR1, HNRNPA2B1, LRPPRC, YTHDC2, YTHDF3, and METTL14 as protective factors significantly associated with overall survival. In contrast, FTO, VIRMA, and ZC3H13 were categorized as risk factors (Figure S1B). Moreover, we assessed the mutual regulation between these m6A regulatory factors through Spearman correlation analysis, examining different chips. The findings highlighted highly correlated expression patterns within the same functional category, as well as significant correlations among writers, erasers, and readers (Figure S1C). These results underscore the intricate cross-talk between writer, reader, and eraser regulatory factors, which plays a crucial role in the occurrence and development of CRC. Moving forward, we extracted the expression matrix of m6A genes and PCD genes from the TCGA-CRC cohort, subjecting it to Spearman correlation analysis. PCD genes that displayed significant correlations with at least one gene in the m6A gene set ($|R| \geq 0.3$ and p value <0.05) were defined as m6A-related PCD genes. In total, 854 m6A-related PCD genes were identified (Figure 1A).

Construction of risk model based on N6-methyladenosine-associated programmed cell death genes

In the TCGA-CRC cohort, we identified a total of 276 differentially expressed genes (DEGs) with adjusted p value <0.05 and $|\log_2 FC| \geq 0.5$. Among these DEGs, 165 genes displayed upregulation, while 111 genes were downregulated in CRC (Figure 1B). Utilizing Cox regression analysis and Kaplan-Meier survival analysis with the TCGA-CRC cohort, we pinpointed 14 m6A-associated PCD genes that exhibited significant associations with overall patient survival (OS) (Figure 1C). Based on the minimum criteria, we selected 10 m6A-associated PCD genes for the prediction model using LASSO Cox regression analysis with the TCGA-CRC data as the training dataset (Figures 1D–1F). Importantly, these genes also showed significant correlations with m6A regulatory factors in other validation datasets (Figure S2A). In the TCGA-CRC cohort, we observed that INHBB, SNAI1, TNFRSF10A, SFPQ, GLA, ITGA6, and TRAP1 were upregulated in CRC, while DAPK1, MTM1, and GSKIP were downregulated (Figure S2B). Further validation of the expression of m6A-associated PCD genes in GSE32323 revealed that all genes, except TNFRSF10A, SFPQ, and ITGA6, displayed consistent expression trends (Figure S2C). Moreover, survival analysis confirmed the association of these genes, with the exception of SFPQ and MTM1, with CRC prognosis in multiple datasets (Figure S2D). We proceeded to validate the expression levels of INHBB and SNAI1 in cell lines and clinical tissue samples using qRT-PCR (Figures 1G and 1H). The results affirmed that INHBB and SNAI1 were upregulated in CRC cell lines and fresh tissue samples, showing a positive correlation with FTO (m6A erasers). These findings were in line with the results from the TCGA-CRC cohort (Figures S2E and S2F).

The cell death-related risk score (CDRS) was then calculated for each patient based on the expression of the 10 selected m6A-related programmed cell death (PCD) genes and their respective regression coefficients (Figure 1F). The formula for calculating CDRS was as follows: CDRS = 0.345 * DAPK1 +0.179 * INHBB +0.067 *SNAI1 - 0.028 * TRAP1 - 0.034 * ITGA6 - 0.046 * GSKIP - 0.068 * GLA - 0.09 * MTM1- 0.111 * SFPQ -0.152 *TNFRSF10A (Figure 1F). Furthermore, we explored the correlation between CDRS and 14 m6A-related PCD genes, as well as 23 m6A genes across five different microarray platforms. The results demonstrated that CDRS was significantly positively correlated with m6A-related PCD genes and m6A genes (Figures S2G and S2H). Conversely, CDRS exhibited significant negative correlations with seven other m6A-related PCD genes, nine "readers," and five "writers" (Figures S2H and S2I). In addition, we found that CDRS was significantly associated with various clinical features, including survival status, gender, T stage, N stage, M stage, and AJCC stage (Figure 1I). Consensus Molecular Subtypes (CMSs) divide CRC into four distinct subtypes based on transcriptome profiling: CMS1 (microsatellite instability immune), CMS2 (canonical), CMS3 (metabolic), and CMS4 (mesenchymal).[29] Notably, patients with CMS4 subtype, who exhibited worse overall survival, displayed the highest CDRS score (Figure 1I).

The cell death-related risk score as an independent risk factor for colorectal cancer

Patients with CRC were stratified into high- and low-CDRS groups based on the median value of CDRS. In both the TCGA-CRC training dataset and other validation datasets, patients in the high-risk group exhibited significantly lower overall survival compared to those in the low-risk

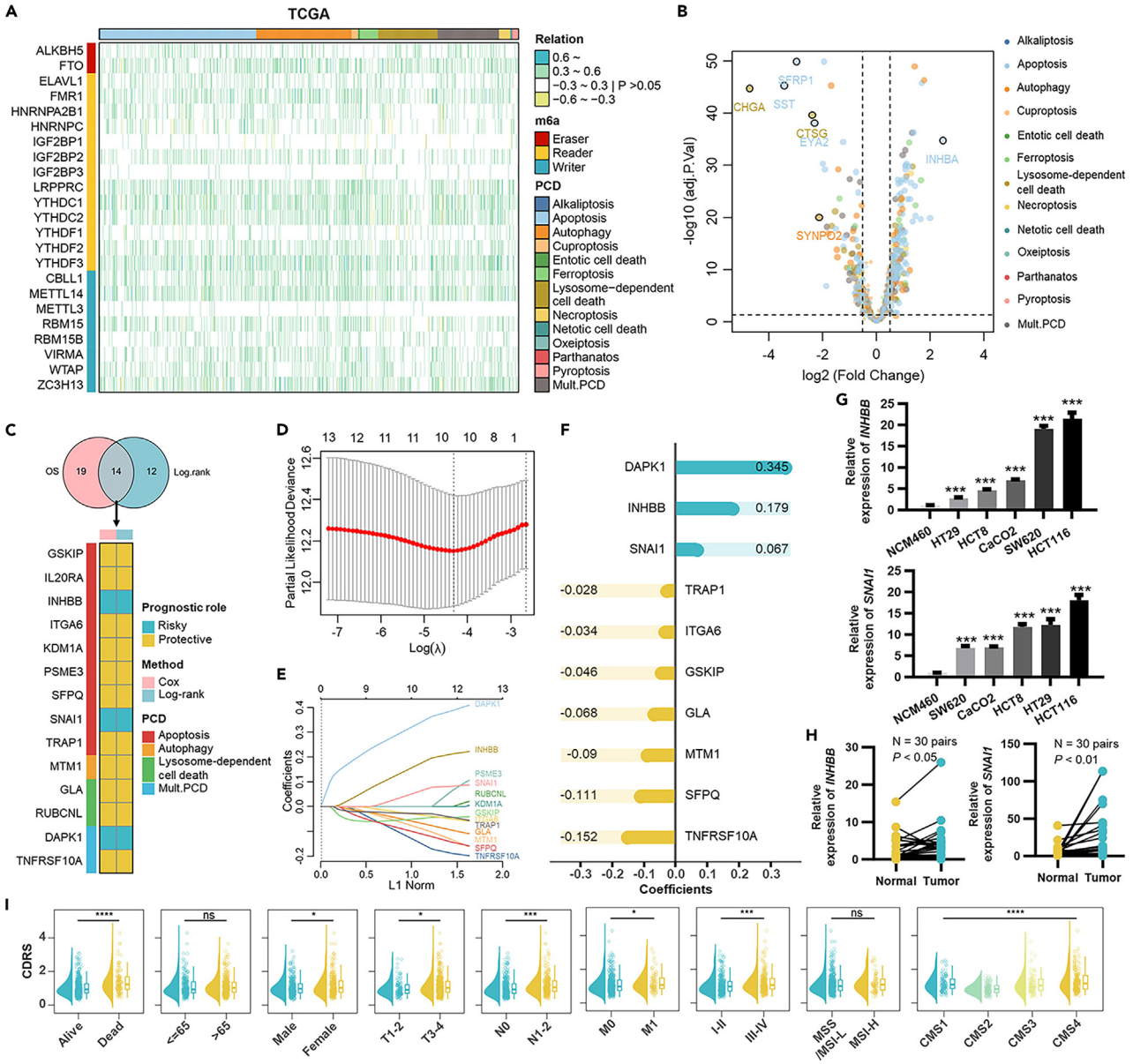

Figure 1. Identification, selection, and validation of m6A-associated PCD genes in patients with colorectal cancer

(A) Correlation analysis between m6A regulatory factors and PCD genes in the TCGA-CRC dataset.

(B) Volcano plot showing differentially expressed m6A-related PCD genes in CRC tumors and normal tissues.

(C) Univariate Cox regression ($p < 0.1$) and Kaplan-Meier survival analysis ($p < 0.01$) of m6A-related PCD genes in the TCGA-CRC dataset. The Venn diagram (top) shows the number of intersection genes between Univariate Cox regression and Kaplan-Meier survival analysis. The heatmap (bottom) further displays the selected genes.

(D and E) LASSO analysis identifies 10 m6A-related PCD genes.

(F) Coefficients of the 10 m6A-related PCD genes finally obtained in LASSO-Cox regression.

(G) qRT-PCR experiments examining the expression of INHBB/SNAI1 genes in CRC cell lines and normal epithelial cell lines.

(H) qRT-PCR experiments examining the expression of INHBB/SNAI1 genes in fresh CRC tissue.

(I) Analysis of the distribution differences of the CDRS in different survival status, age, gender, T, N, M, AJCC stage, MSI, and consensus molecular subtypes. (*$p < 0.05$; ***$p < 0.001$; ****$p < 0.0001$; ns, $p > 0.05$).

group (Figure 2A). To assess the independent prognostic value of CDRS, univariate and multivariate Cox analyses were performed (Figures 2B and 2C). The results of the univariate analysis indicated a significant correlation between high CDRS and reduced overall survival, with HR > 1 in all datasets (Figure 2B). After adjusting for available clinical characteristics, such as age, gender, T stage, N stage, M stage, AJCC stage, and

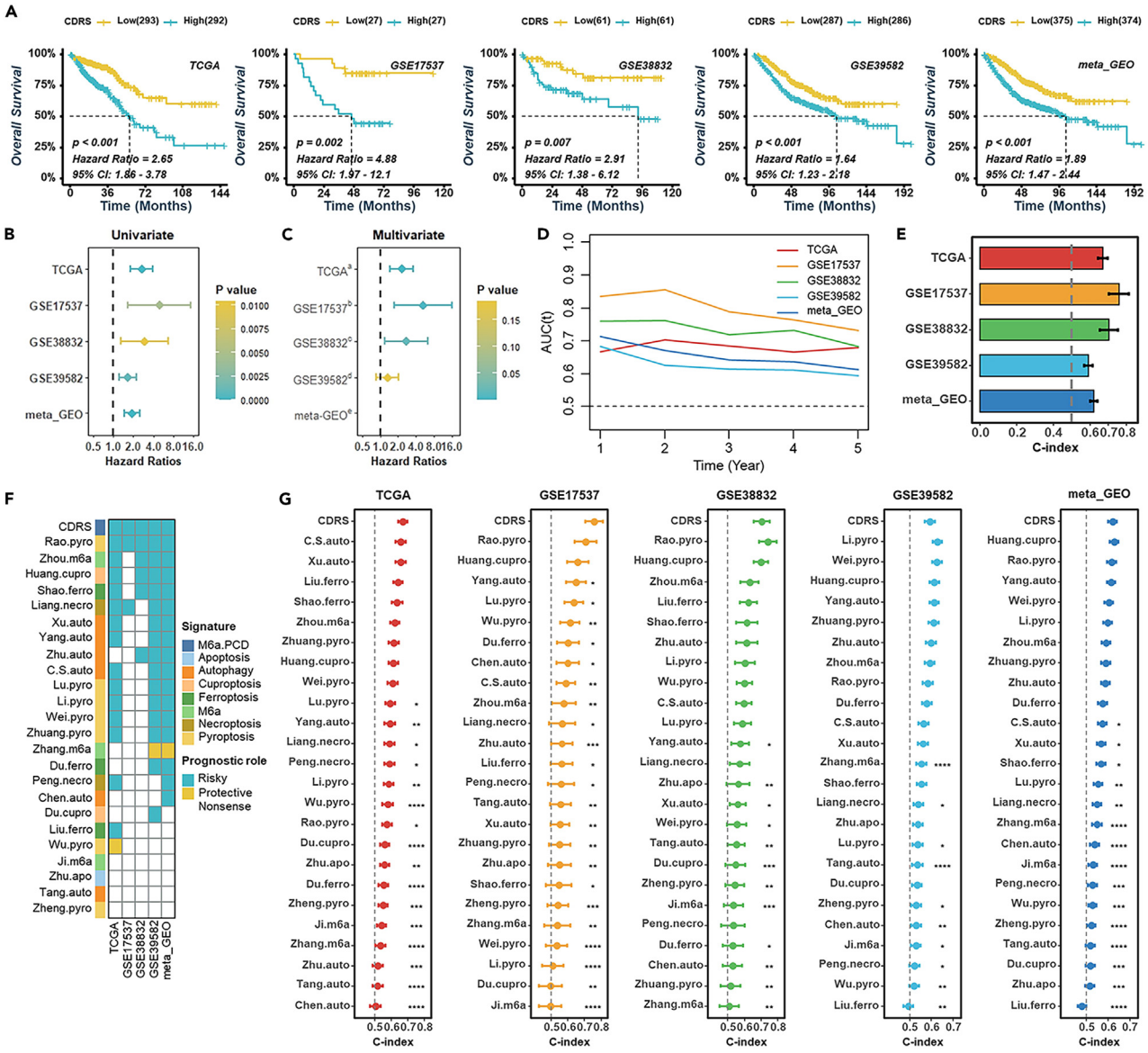

Figure 2. Prognostic evaluation and comparison of CDRS in patients with CRC

(A) Kaplan-Meier survival curves of OS in patients with high and low CDRS scores in multiple datasets.

(B) Univariate Cox regression analysis of the association between CDRS and CRC prognosis in multiple datasets.

(C) Multivariate Cox regression analysis of the association between CDRS and CRC prognosis in multiple datasets, with adjustment for different factors.

(D) AUCs based on CDRS for different durations of OS in multiple datasets.

(E) The C-index of CDRS in TCGA, GSE17537, GSE38832, GSE39582, and *meta*-GEO.

(F) Univariate Cox regression analysis of CDRS and other m6A/PCD-related signatures in multiple datasets.

(G) The C-index of CDRS and other m6A/PCD-related signatures in TCGA, GSE17537, GSE38832, GSE39582, and *meta*-GEO. (*p < 0.05; **p < 0.01; ***p < 0.001; ****p < 0.0001).

microsatellite state, the multivariate analysis revealed that CDRS remained a statistically significant and independent prognostic factor (Figure 2C). Furthermore, time-dependent AUC and c-index analyses demonstrated that CDRS consistently displayed robust performance across multiple independent cohorts (Figures 2D and 2E). In comparison with other clinical characteristics (age, gender, T, N, M, AJCC stage, MSI, TMB, ACT) and molecular variables (TP53, KRAS, and BRAF), CDRS exhibited superior predictive accuracy over age, gender, T stage, MSI, TMB, TP53, KRAS, and BRAF, and was on par with N, M, and AJCC stage (Figure S3A). Given the existence of several prognostic models based on m6A or individual mortality patterns in CRC, we further compared the performance of CDRS with other signatures for predicting CRC prognosis. Univariate Cox regression, C-index, and AUC analyses across TCGA and GEO datasets consistently demonstrated that CDRS

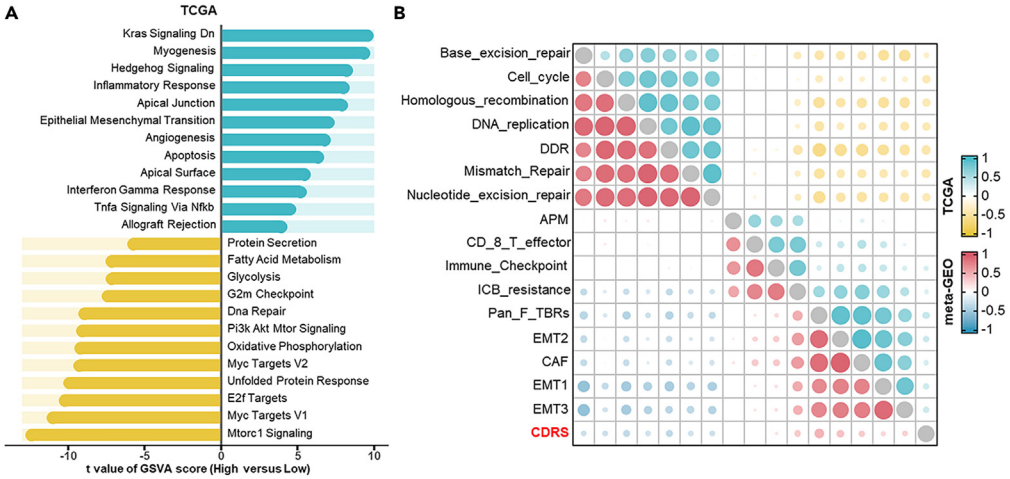

Figure 3. Impact of CDRS on biological pathways and cancer-related signatures

(A) Gene Set Variation Analysis (GSVA) was performed using hallmark gene sets in patients with low- and high-CDRS scores from the TCGA-CRC dataset.

(B) Correlation analysis was conducted between CDRS and various cancer-related signatures in the TCGA-CRC and *meta*-GEO datasets.

outperformed other signatures (Figures 2F, 2G, and S3B; Table S2). To enhance the accuracy of predicting overall survival among individuals with CRC, we used multivariable Cox regression to establish a nomogram model in the TCGA cohort to estimate the 1-, 3-, and 5-year overall survival. The model included age, M, AJCC stage, and CDRS (Figure S3C). The calibration curves confirmed the accuracy of the nomogram in predicting 1-, 3-, and 5-year overall survival (Figure S3D). Furthermore, decision curve analysis (DCA) demonstrated that the nomogram model surpassed other predictors used in this study (Figure S3E).

Biological pathways associated with the cell death-related risk score signature

The remarkable prognostic capability of CDRS in predicting CRC outcomes has sparked our curiosity in understanding the underlying mechanisms. To delve into these mechanisms, we employed Gene Set Variation Analysis (GSVA) to explore the impact of CDRS on biological pathways across all datasets.

Our analysis revealed that the high CDRS group exhibited the activation of stromal and inflammation-related pathways, including but not limited to epithelial mesenchymal transition (EMT), angiogenesis, apical junction, inflammatory response, and interferon gamma response. In contrast, the low CDRS group displayed the upregulation of pathways associated with cell growth and pro-cancer mechanisms, including DNA repair, G2M checkpoint, PI3K/AKT/mTOR signaling, and Wnt/Beta-Catenin signaling (Figure 3A and S4A–S4D). Furthermore, our findings suggested that EMT, angiogenesis, and stromal-relevant signatures were more prominent in the high INHBB/SNAI1 expression group (Figure S5A). Additionally, correlation analysis established a positive association between CDRS and stromal-relevant signatures such as EMT1/2/3, cancer-associated fibroblasts (CAFs), and the pan-fibroblast signature (PAN-F-TBR), while displaying a negative correlation with pathways related to cell growth (Figure 3B). Although CDRS did not exhibit any significant correlation with CD8 T effector and antigen processing machinery (APM) signatures, it displayed a negative correlation with signals associated with resistance to immune checkpoint blockade (ICB) (Figure 3B).

Genomic features of different cell death-related risk score groups

We then proceeded to compare somatic mutations and copy number alterations between the high and low CDRS groups, but the results revealed no significant differences between the two groups (Figures S6A and S6B). Using Fisher's exact test with a threshold of $p < 0.01$, we identified 24 differently mutated genes. Although the mutation rate of these genes was low, we observed that the low CDRS group had a higher frequency of APC mutations, whereas the high CDRS group exhibited a higher frequency of BRAF mutations (Figure 4A). In both the TCGA-CRC and GSE39582 datasets, the BRAF mutation group had a higher CDRS, while no significant difference in CDRS was observed between wild-type and mutated groups for KRAS and TP53 (Figure 4B).

Association of cell death-related risk score with the immune microenvironment

Given the significant association between CDRS and certain stromal-relevant signatures, we conducted an extensive investigation into the relationship between CDRS and the tumor microenvironment. First, we utilized the ESTIMATE algorithm to calculate the stromal score and immune score in the TCGA-CRC and *meta*-GEO datasets. Our findings indicated that the CDRS signature was positively correlated with the stromal score, immune score, and ESTIMATE score (the integration of the stromal score and immune score), while it was negatively correlated with tumor purity (Figure 5A). Next, we employed the EPIC method to quantify immune cell infiltration in TCGA-CRC. Notably,

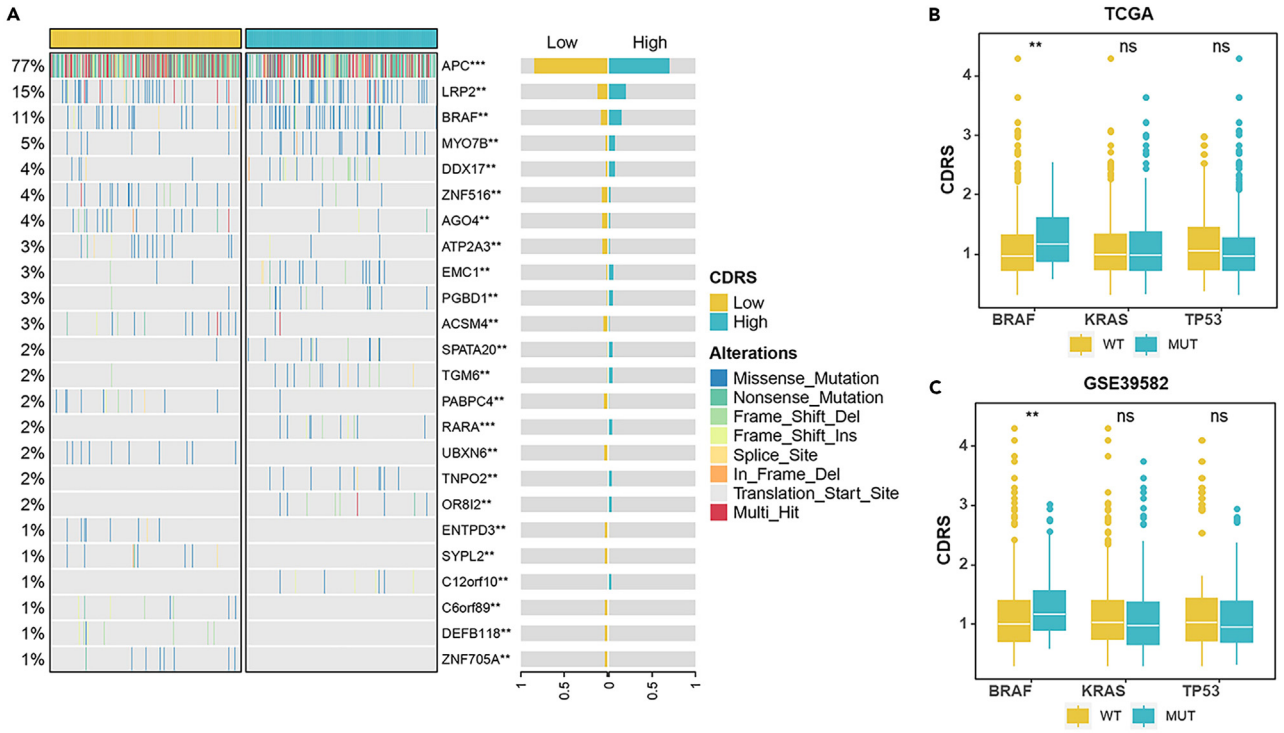

Figure 4. Somatic mutations and association with CDRS scores in CRC

(A) Mutational landscape (left) and frequency (right) of genes with different somatic mutations between high- and low-CDRS groups.

(B and C) Distribution of CDRS scores in groups with mutated and wild-type BRAF/KRAS/TP53 in TCGA-CRC (B) and GSE39582 datasets (C). (**$p < 0.01$; ***$p < 0.001$; ns, $p > 0.05$).

critical components of the stromal microenvironment, such as cancer-associated fibroblasts (CAFs) and epithelial cells, exhibited a clear positive correlation with CDRS (Figure S7A). Moreover, CDRS showed a significant association with macrophages (Figure S7A). Macrophages, especially tumor-associated macrophages (TAMs), are considered to be vital tumor-infiltrating immune cells involved in the complex interplay between tumor cells and the tumor microenvironment (TME).[30] To further assess immune cell infiltration, we utilized various algorithms including EPIC, MCP-COUNTER, XCELL, TIDE, CIBERSORT, and QUANTISEQ. The results showed that CDRS was positively correlated with CAFs, epithelial cells, and M2-like macrophages (Figure 5B). Additionally, m6A-related PCD genes, DAPK1, INHBB, and SNAI1, displayed positive correlations with CAFs, epithelial cells, and M2-like macrophages, whereas GSKIO, ITGA6, and TRAP1 exhibited the opposite trend (Figure S7B). Transforming growth factor β (TGF-β) is known to be a significant regulator of CAF activation.[31,32] Patients with high CDRS exhibited higher TGF-β signaling compared to those with low CDRS (Figures 5C and S7C). Additionally, we investigated the correlation between immunomodulators and CDRS values and observed that CDRS was primarily positively correlated with TGFB1 (Figure S7D). Furthermore, macrophage-related chemokines, CCL5 and CX3CL1, were highly expressed in the high CDRS group (Figure S7D). Using the TIDE method, we found that the high CDRS group had higher TIDE, exclusion score (only in the *meta*-GEO dataset), and dysfunction score in both the TCGA-CRC and *meta*-GEO cohorts (Figures 5D and 5E). The IPS algorithm also revealed that high CDRS was associated with a lower IPS, indicating lower immunogenicity (Figure S7E). In the IMvigor210 cohort, although the immune desert and immune-excluded phenotypes had higher CDRS (Figure S7F), CDRS was not significantly associated with patient prognosis (Figure S7G).

The role of cell death-related risk score in predicting drug sensitivity

To investigate the relationship between CDRS and drug sensitivity, we utilized large-scale drug sensitivity and gene expression data from hundreds of cancer cell lines (CCLs) in the Cancer Therapeutics Response Portal (CRPT) and Profiling Relative Inhibition Simultaneously in Mixtures (PRISM) datasets to establish a predictive model for drug response (Figure 6A). Using gene expression profiles, we estimated the AUC values of each compound in each clinical sample by employing a ridge regression model via the "pRRophetic" package. AUC values were found to be negatively correlated with drug sensitivity. The detailed workflow is shown in Figure 6A. First, we performed differential drug response analysis ($|log2FC| > 0.10$) between the high-CDRS (top decile) and low-CDRS (bottom decile) groups to identify compounds with the most significant differences in AUC values (Figure 6A). Next, we filtered the compounds by calculating Spearman correlation between AUC values and CDRS and selecting compounds with a correlation coefficient of Spearman's $|R| > 0.30$ for both CTRP and PRISM (Figure 6A). Finally, we identified 10 CTRP-derived compounds and 11 PRISM-derived compounds (Figures 6B and 6C). One of the compounds, Dasatinib,

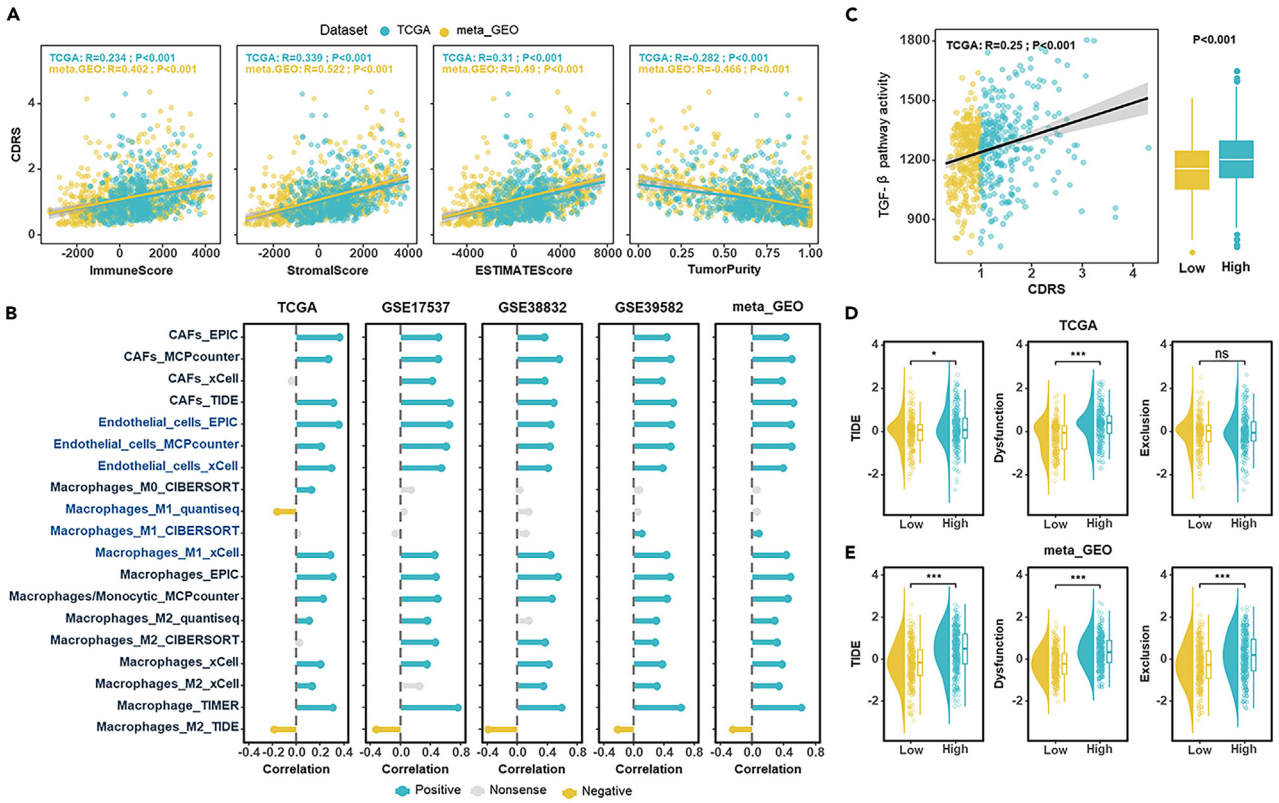

Figure 5. Relationship between CDRS and tumor microenvironment in CRC

(A) Correlation analysis between CDRS and immune score, stromal score, ESTIMATE score, and tumor purity in TCGA-CRC and meta-data datasets.

(B) Analysis of the correlation between CDRS and CAFs, epithelial cells, and macrophages using EPIC, MCP-COUNTER, XCELL, TIDE, CIBERSORT, and QUANTISEQ algorithms in multiple datasets. (C) Analysis of the correlation between TGF-β and CDRS in TCGA-CRC datasets (left) and distribution of TGF-β signaling in high- and low-CDRS groups (right).

(D and E) Distribution of TIDE score (left), exclusion score (middle), and dysfunction score (right) in different CDRS groups in TCGA-CRC (D) and meta-data datasets (E). (*p < 0.05; ***p < 0.001; ns, p > 0.05).

is an orally bioavailable and promising therapeutic drug used to treat various human malignancies, although it's relatively specific for ABL, BCR-ABL, and the SFKs. Dasatinib has been shown to sensitize KRAS mutant colorectal tumors to cetuximab.[33] Although CDRS did not show a significant difference between KRAS mutant and patients with wild-type colorectal cancer, you found that the high-CDRS group had lower estimated AUC values for Dasatinib (Figures 6B and 6C). Similarly, five other drugs (romidepsin, panobinostat, vindesine, YM-155, echinomycin) also showed lower estimated AUC values in the high-CDRS group, suggesting that they may be potential therapeutic options for patients with CRC with high CDRS (Figures 6B and 6C).

DISCUSSION

To our knowledge, this study represents the first comprehensive analysis of the role of m6A-related programmed cell death (PCD) genes in risk stratification and the management of colorectal cancer (CRC). We constructed a 10-gene prognostic signature consisting of DAPK1, INHBB, SNAI1, TNFRSF10A, SFPQ, MTM1, GLA, GSKIP, ITGA6, and TRAP1 in the TCGA-CRC cohort. Importantly, we further validated the signature's stable performance in three external cohorts (GSE17537, GSE38832, GSE39582). The proposed Cell Death-Related Score (CDRS) is not only an independent risk factor for CRC but also plays a vital role in the tumor microenvironment (TME) as suggested by pathway analysis. Additionally, we explored the association between CDRS and drug sensitivity, leading to the identification of six potential therapeutic drugs for patients with CRC with high CDRS. These findings offer novel insights for personalized prediction methods and precision treatment of CRC.

As the field of cancer treatment evolves toward precision medicine, numerous studies aim to accurately assess patient survival using various approaches. Traditional clinical and pathological features, such as tumor size,[34] C-reactive protein,[35] and lymph node metastasis,[36] have been established as independent prognostic factors for CRC. However, the high genetic and genomic diversity among patients with CRC renders these factors less effective in predicting survival.[37,38] Recent research has shown that developing gene signatures based on large-scale gene expression datasets holds great promise for assessing cancer patient survival.[39,40] In the context of CRC, multiple prognostic

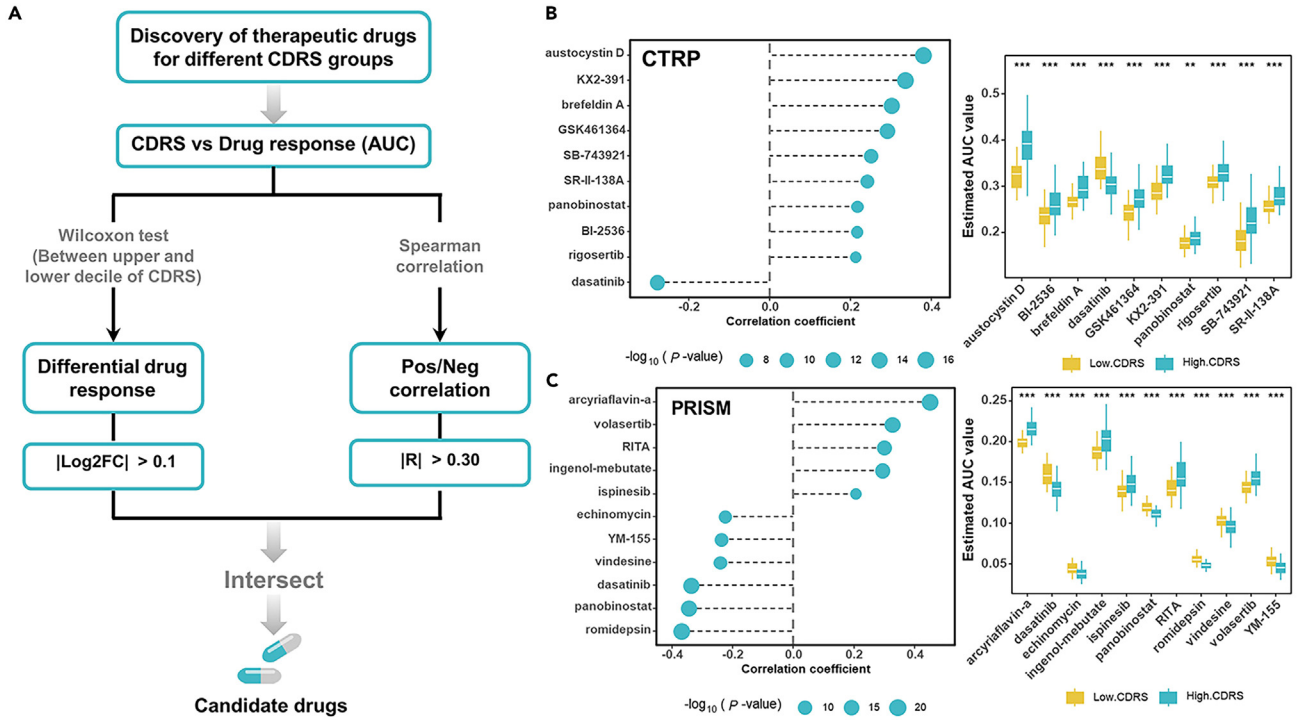

Figure 6. Identification of highly sensitive drugs based on CDRS

(A) Strategies for identifying highly sensitive drugs in patients with different CDRS scores.

(B and C) Correlation analysis (left) and distribution in low and high CDRS groups (right) of the AUC values of 10 CTRP-derived compounds (B) and 11 PRISM-derived compounds with CDRS (C). (**p < 0.01; ***p < 0.001).

gene models with significant clinical value have been established.[10,41] It has been reported that m6A plays an increasingly important role in various physiological and pathological processes in various cancers,[42] including pancreatic cancer,[43] breast cancer,[44] and our published CRC study.[45] While the roles of various programmed cell death (PCD) modes in CRC prognosis have been explored in the literature, these models have primarily focused on individual modes of cell death, such as the apoptosis-related prognostic signature,[46] autophagy-related signature,[47–51] cuproptosis-related signature,[52–54] ferroptosis-related signature,[55–57] necroptosis-related signature,[58,59] and pyroptosis-related prognostic signature.[60–65] However, the interplay between m6A modification and PCD in CRC prognosis remains unexplored, representing a gap in the existing literature. In this study, we identified 854 m6A-related PCD genes through Pearson correlation analysis and then selected 10 prognosis-related genes through univariate and multivariate Cox proportional hazard regression. Among them, INHBB is a member of the transforming growth factor β superfamily, which has been identified as a potential prognostic biomarker in various cancers including CRC.[66,67] We also found that INHBB was highly expressed in CRC, but the expression trend lacked necessary experimental verification and was only predicted by bioinformatics analysis. SNAI1 is a critical EMT inducer and a driving factor for cancer progression, including cell invasion, survival, immune regulation, stemness, and metabolic regulation. It is closely related to m6A and affects tumor metastasis.[68,69] A large number of studies have reported its pro-cancer role in CRC.[70,71] Our study used qRT-PCR to confirm the expression levels of INHBB and SNAI1 in CRC cell lines and clinical tissue samples, which were found to be positively correlated with FTO, one of the m6A erasers, consistent with our TCGA-CRC results. Our results further demonstrated that the Cell Death-Related Score (CDRS), derived from these 10 genes, serves as an independent risk factor for CRC. CDRS outperformed age, gender, T stage, MSI, TMB, TP53, KRAS, and BRAF in predicting prognosis, demonstrating its superiority to common clinical variables. Moreover, patients with the CMS4 subtype, characterized by poor overall survival, exhibited the highest CDRS scores. In addition, we compared the performance of CDRS with other existing signatures for predicting CRC prognosis. Our study, supported by univariate Cox regression, C-index, and AUC analyses, revealed that CDRS outperformed all other signatures, establishing it as a robust predictor of CRC survival across both TCGA and GEO datasets.

Exploration of CDRS and tumor-related biological pathways revealed that the high CDRS group exhibited the activation of stromal-relevant signatures and inflammation-related pathways, while the low CDRS group showed the upregulation of cell growth and pro-cancer pathways. Studies have shown that EMT plays a critical role in tumor invasion and metastasis.[72] Our results may suggest that high CDRS is closely related to tumor metastasis and invasion, while low CDRS may promote tumor growth. This observation aligns with the functionality of the genes in our model. For instance, SFPQ has been reported to promote cancer progression through various mechanisms such as RNA transcriptional activity, mRNA processing, splice regulation, and innate immune response in ovarian cancer,[73] breast cancer,[74] liver cancer,[75] and colorectal cancer.[76] In colorectal cancer, SFPQ has been shown to promote proliferation and the development of the disease.[76] TNFRSF10A,

another gene in the CDRS signature, encodes a protein within the tumor necrosis factor (TNF) receptor superfamily. It has been linked to the promotion of colorectal cancer by upregulating HuR.[77] TRAP1, or TNF receptor-associated protein 1, plays a role in regulating cell cycle and apoptosis in thyroid cancer cells.[78] ITGA6, which encodes a member of the integrin alpha chain protein family, has been associated with the occurrence and development of bladder cancer through the m6A modification of ITGA6 mRNA.[79] Furthermore, EMT can be triggered by imbalanced ECM,[80] and CAFs are an important component of the ECM.[81] Our study revealed a positive correlation between CDRS and CAFs, emphasizing the critical role of CAFs in the extracellular matrix. Transforming growth factor β (TGF-β), a well-known regulator of CAF activation,[31,32] was found to be higher in patients with high CDRS, providing further insights into the interaction between CDRS and the TME.

As is widely known, CAFs and ECM are crucial components of the TME. The permissive TME often enables tumor cells to evade immune surveillance and resist drug interference.[82] Our findings highlight that the expression pattern of CDRS significantly correlates with immune responses and suggest the potential impact of CDRS on CRC progression by influencing immune-related gene regulatory networks. This study adds to our understanding by revealing that the CDRS signature positively correlates with the stromal score, immune score, and ESTIMATE score, while negatively impacting tumor purity. Previously, it has been reported that SNAI1 is involved in tumor immune evasion by inducing chemokines and immune suppressive cells into the TME.[69] TAMs, specifically M2-TAMs, are pivotal in tumor progression,[30,83] and our results show a positive correlation between CDRS and M2-like macrophages. Moreover, our study highlights that the m6A-related PCD genes, such as DAPK1, INHBB, and SNAI1, are positively correlated with CAFs, epithelial cells, and M2-like macrophages, while GSKIO, ITGA6, and TRAP1 show the opposite trend. Previous studies have shown that the enrichment of M2-like macrophages indicates a poor prognosis in the tumor microenvironment of triple-negative breast cancer,[84] which is consistent with our prediction of CRC prognosis. To date, our study is the first t systematically elucidate the prognostic value of m6A-related PCD genes and their regulatory role in the anti-tumor immune response in patients with CRC.

Moreover, our current research proposes for the first time the clinical application of CDRS in CRC, which may help in formulating different treatment strategies. By examining drug sensitivity, we have identified that patients in the high CDRS group may be more responsive to specific drugs, including dasatinib, romidepsin, panobinostat, vindesine, YM-155, and echinomycin. This finding holds promise for guiding personalized treatment strategies based on CDRS, potentially improving the survival rates of patients with CRC by tailoring therapies to individual profiles.

In summary, we conducted a comprehensive analysis using large-scale clinical samples and transcriptome data to develop a 10-gene risk signature based on m6A-related PCD genes. This signature effectively predicts survival outcomes and drug sensitivity in patients with CRC. While these findings require validation in human CRC models, they hold the potential to serve as novel prognostic biomarkers and provide new insights for personalized prediction methods and precision treatment in CRC.

Limitations of the study

Despite the promising performance of our model in both training and validation cohorts, there are several limitations to this study. First, the available CRC samples and clinical follow-up data are not extensive enough for internal validation, necessitating further cohort studies to confirm the applicability of our prognostic prediction model. Second, the specific molecular mechanisms and biological functions of the ten m6A-related PCD genes in CRC remain unclear, highlighting the need for further experimental research. Before our clinical model can be applied in practice, additional multicenter randomized controlled trials with high-quality data, large sample sizes, and extended follow-up periods are essential for further validation. Additionally, although we used CTRP and PRISM for potential drug predictions based on different CDRS values, these results lack experimental validation.

STAR★METHODS

Detailed methods are provided in the online version of this paper and include the following:

- KEY RESOURCES TABLE
- RESOURCE AVAILABILITY
  - Lead contact
  - Materials availability
  - Data and code availability
- EXPERIMENTAL MODEL AND SUBJECT DETAILS
  - Cell lines
  - Human tissue specimens
- METHOD DETAILS
  - Data retrieval and preprocessing
  - Screening for m6A-associated PCD genes
  - Construction of the risk score model
  - Functional enrichment analysis
  - Tumor microenvironment analysis
  - RNA extraction and real-time quantitative PCR (qPCR)

- Potential therapeutic agents
- Statistical analysis

SUPPLEMENTAL INFORMATION

Supplemental information can be found online at https://doi.org/10.1016/j.isci.2023.108720.

ACKNOWLEDGMENTS

We would like to thank GEO, TCGA database and IMvigor210 cohort, as well as all those who have shared their data on the platforms. This work received support from the National Natural Science Foundation of China (No. 82373062), the Outstanding Youth Foundation of Hunan Provincial Natural Science Foundation of China (No. 2022JJ20098), and the Central South University Innovation-Driven Research Program (No. 2023CXQD075). This study was reviewed and approved by the Ethics Committee of Xiangya Hospital Central South University and conducted under the guidance of the Declaration of Helsinki.

AUTHOR CONTRIBUTIONS

Y.L., Q.W. and X.F. conceived the work and analyzed the data. Q.W. and X.F. drafted the article. C.O. provided the funds. J.L., X.F. and C.O. edited and revised the article. All authors have read and agreed to the final version of the article.

DECLARATION OF INTERESTS

The authors declare no potential conflicts of interest.

INCLUSION AND DIVERSITY

We support inclusive, diverse, and equitable conduct of research.

Received: July 15, 2023
Revised: October 30, 2023
Accepted: December 11, 2023
Published: December 13, 2023

REFERENCES

1. Siegel, R.L., Miller, K.D., Wagle, N.S., and Jemal, A. (2023). Cancer statistics, 2023. CA. Cancer J. Clin. *73*, 17–48.
2. Sung, H., Ferlay, J., Siegel, R.L., Laversanne, M., Soerjomataram, I., Jemal, A., and Bray, F. (2021). Global Cancer Statistics 2020: GLOBOCAN Estimates of Incidence and Mortality Worldwide for 36 Cancers in 185 Countries. CA. Cancer J. Clin. *71*, 209–249.
3. Li, Y., Gan, Y., Liu, J., Li, J., Zhou, Z., Tian, R., Sun, R., Liu, J., Xiao, Q., Li, Y., et al. (2022). Downregulation of MEIS1 mediated by ELFN1-AS1/EZH2/DNMT3a axis promotes tumorigenesis and oxaliplatin resistance in colorectal cancer. Signal Transduct. Target. Ther. *7*, 87.
4. Li, Y., Liu, J., Xiao, Q., Tian, R., Zhou, Z., Gan, Y., Li, Y., Shu, G., and Yin, G. (2020). EN2 as an oncogene promotes tumor progression via regulating CCL20 in colorectal cancer. Cell Death Dis. *11*, 604.
5. Ciardiello, D., Guerrera, L.P., Maiorano, B.A., Parente, P., Latiano, T.P., Di Maio, M., Ciardiello, F., Troiani, T., Martinelli, E., and Maiello, E. (2022). Immunotherapy in advanced anal cancer: Is the beginning of a new era? Cancer Treat Rev. *105*, 102373.
6. Miller, K.D., Nogueira, L., Devasia, T., Mariotto, A.B., Yabroff, K.R., Jemal, A., Kramer, J., and Siegel, R.L. (2022). Cancer treatment and survivorship statistics. CA. Cancer J. Clin. *72*, 409–436.
7. Tan, L., Qin, Y., Xie, R., Xia, T., Duan, X., Peng, L., You, R., Liu, Y., Zou, X., Zhang, M., et al. (2022). N6-methyladenosine-associated prognostic pseudogenes contribute to predicting immunotherapy benefits and therapeutic agents in head and neck squamous cell carcinoma. Theranostics *12*, 7267–7288.
8. Zou, Y., Xie, J., Zheng, S., Liu, W., Tang, Y., Tian, W., Deng, X., Wu, L., Zhang, Y., Wong, C.W., et al. (2022). Leveraging diverse cell-death patterns to predict the prognosis and drug sensitivity of triple-negative breast cancer patients after surgery. Int. J. Surg. *107*, 106936.
9. Li, D., Shi, Z., Liu, X., Jin, S., Chen, P., Zhang, Y., Chen, G., Fan, X., Yang, J., and Lin, H. (2023). Identification and development of a novel risk model based on cuproptosis-associated RNA methylation regulators for predicting prognosis and characterizing immune status in hepatocellular carcinoma. Hepatol. Int. *17*, 112–130.
10. Zhou, L., Yu, Y., Wen, R., Zheng, K., Jiang, S., Zhu, X., Sui, J., Gong, H., Lou, Z., Hao, L., et al. (2022). Development and Validation of an 8-Gene Signature to Improve Survival Prediction of Colorectal Cancer. Front. Oncol. *12*, 863094.
11. Lim, S.H., Cho, H.J., Kim, K.M., Lim, H.Y., Kang, W.K., Lee, J., Park, Y.S., Kim, H.C., and Kim, S.T. (2023). Comprehensive molecular analysis to predict the efficacy of chemotherapy containing bevacizumab in patients with metastatic colorectal cancer. Oncol. Res. *31*, 855–866.
12. Han, Y., Wang, D., Peng, L., Huang, T., He, X., Wang, J., and Ou, C. (2022). Single-cell sequencing: a promising approach for uncovering the mechanisms of tumor metastasis. J. Hematol. Oncol. *15*, 59.
13. Liu, L., Li, H., Hu, D., Wang, Y., Shao, W., Zhong, J., Yang, S., Liu, J., and Zhang, J. (2022). Insights into N6-methyladenosine and programmed cell death in cancer. Mol. Cancer *21*, 32.
14. Wang, D., Han, Y., Peng, L., Huang, T., He, X., Wang, J., and Ou, C. (2023). Crosstalk between N6-methyladenosine (m6A) modification and noncoding RNA in tumor microenvironment. Int. J. Biol. Sci. *19*, 2198–2219.
15. Wang, X., Lu, Z., Gomez, A., Hon, G.C., Yue, Y., Han, D., Fu, Y., Parisien, M., Dai, Q., Jia, G., et al. (2014). N6-methyladenosine-dependent regulation of messenger RNA stability. Nature *505*, 117–120.
16. Yin, H., Zhang, X., Yang, P., Zhang, X., Peng, Y., Li, D., Yu, Y., Wu, Y., Wang, Y., Zhang, J., et al. (2021). RNA m6A methylation orchestrates cancer growth and metastasis via macrophage reprogramming. Nat. Commun. *12*, 1394.
17. Yang, Y., Hsu, P.J., Chen, Y.S., and Yang, Y.G. (2018). Dynamic transcriptomic m(6)A decoration: writers, erasers, readers and functions in RNA metabolism. Cell Res. *28*, 616–624.

18. Zaccara, S., Ries, R.J., and Jaffrey, S.R. (2019). Reading, writing and erasing mRNA methylation. Nat. Rev. Mol. Cell Biol. *20*, 608–624.
19. Shi, H., Wei, J., and He, C. (2019). When, and How: Context-Dependent Functions of RNA Methylation Writers, Readers, and Erasers. Mol. Cell *74*, 640–650.
20. He, L., Li, H., Wu, A., Peng, Y., Shu, G., and Yin, G. (2019). Functions of N6-methyladenosine and its role in cancer. Mol. Cancer *18*, 176.
21. Lan, Q., Liu, P.Y., Bell, J.L., Wang, J.Y., Hüttelmaier, S., Zhang, X.D., Zhang, L., and Liu, T. (2021). The Emerging Roles of RNA m(6)A Methylation and Demethylation as Critical Regulators of Tumorigenesis, Drug Sensitivity, and Resistance. Cancer Res. *81*, 3431–3440.
22. Gu, Y., Wu, X., Zhang, J., Fang, Y., Pan, Y., Shu, Y., and Ma, P. (2021). The evolving landscape of N(6)-methyladenosine modification in the tumor microenvironment. Mol. Ther. *29*, 1703–1715.
23. Shen, C., Xuan, B., Yan, T., Ma, Y., Xu, P., Tian, X., Zhang, X., Cao, Y., Ma, D., Zhu, X., et al. (2020). m(6 A-dependent glycolysis enhances colorectal cancer progression. Mol. Cancer *19*, 72.
24. Li, W., Gao, Y., Jin, X., Wang, H., Lan, T., Wei, M., Yan, W., Wang, G., Li, Z., Zhao, Z., and Jiang, X. (2022). Comprehensive analysis of N6-methylandenosine regulators and m6A-related RNAs as prognosis factors in colorectal cancer. Mol. Ther. Nucleic Acids *27*, 598–610.
25. Bedoui, S., Herold, M.J., and Strasser, A. (2020). Emerging connectivity of programmed cell death pathways and its physiological implications. Nat. Rev. Mol. Cell Biol. *21*, 678–695.
26. Tang, D., Kang, R., Berghe, T.V., Vandenabeele, P., and Kroemer, G. (2019). The molecular machinery of regulated cell death. Cell Res. *29*, 347–364.
27. Fan, A., Wang, B., Wang, X., Nie, Y., Fan, D., Zhao, X., and Lu, Y. (2021). Immunotherapy in colorectal cancer: current achievements and future perspective. Int. J. Biol. Sci. *17*, 3837–3849.
28. Tang, F., Chen, L., Gao, H., Xiao, D., and Li, X. (2022). m(6)A: An Emerging Role in Programmed Cell Death. Front. Cell Dev. Biol. *10*, 817112.
29. Guinney, J., Dienstmann, R., Wang, X., de Reyniès, A., Schlicker, A., Soneson, C., Marisa, L., Roepman, P., Nyamundanda, G., Angelino, P., et al. (2015). The consensus molecular subtypes of colorectal cancer. Nat. Med. *21*, 1350–1356.
30. He, X., Chen, H., Zhong, X., Wang, Y., Hu, Z., Huang, H., Zhao, S., Wei, P., Shi, D., and Li, D. (2023). BST2 induced macrophage M2 polarization to promote the progression of colorectal cancer. Int. J. Biol. Sci. *19*, 331–345.
31. Tauriello, D.V.F., Palomo-Ponce, S., Stork, D., Berenguer-Llergo, A., Badia-Ramentol, J., Iglesias, M., Sevillano, M., Ibiza, S., Cañellas, A., Hernando-Momblona, X., et al. (2018). TGFbeta drives immune evasion in genetically reconstituted colon cancer metastasis. Nature *554*, 538–543.
32. Pan, H., Pan, J., and Wu, J. (2022). Development and validation of a cancer-associated fibroblast-derived lncRNA signature for predicting clinical outcomes in colorectal cancer. Front. Immunol. *13*, 934221.
33. Dunn, E.F., Iida, M., Myers, R.A., Campbell, D.A., Hintz, K.A., Armstrong, E.A., Li, C., and Wheeler, D.L. (2011). Dasatinib sensitizes KRAS mutant colorectal tumors to cetuximab. Oncogene *30*, 561–574.
34. Ye, H., Zheng, B., Zheng, Q., and Chen, P. (2021). Influence of Old Age on Risk of Lymph Node Metastasis and Survival in Patients With T1 Colorectal Cancer: A Population-Based Analysis. Front. Oncol. *11*, 706488.
35. Zhou, J., Wei, W., Hou, H., Ning, S., Li, J., Huang, B., Liu, K., and Zhang, L. (2021). Prognostic Value of C-Reactive Protein, Glasgow Prognostic Score, and C-Reactive Protein-to-Albumin Ratio in Colorectal Cancer. Front. Cell Dev. Biol. *9*, 637650.
36. Sun, Z.Q., Ma, S., Zhou, Q.B., Yang, S.X., Chang, Y., Zeng, X.Y., Ren, W.G., Han, F.H., Xie, X., Zeng, F.Y., et al. (2017). Prognostic value of lymph node metastasis in patients with T1-stage colorectal cancer from multiple centers in China. World J. Gastroenterol. *23*, 8582–8590.
37. Zygulska, A.L., and Pierzchalski, P. (2022). Novel Diagnostic Biomarkers in Colorectal Cancer. Int. J. Mol. Sci. *23*, 852.
38. Gallois, C., Pernot, S., Zaanan, A., and Taieb, J. (2018). Colorectal Cancer: Why Does Side Matter? Drugs *78*, 789–798.
39. Supplitt, S., Karpinski, P., Sasiadek, M., and Laczmanska, I. (2021). Current Achievements and Applications of Transcriptomics in Personalized Cancer Medicine. Int. J. Mol. Sci. *22*, 1422.
40. Doultsinos, D., and Mills, I.G. (2021). Derivation and Application of Molecular Signatures to Prostate Cancer: Opportunities and Challenges. Cancers *13*, 495.
41. Ahluwalia, P., Kolhe, R., and Gahlay, G.K. (2021). The clinical relevance of gene expression based prognostic signatures in colorectal cancer. Biochim. Biophys. Acta. Rev. Cancer *1875*, 188513.
42. Huang, H., Weng, H., and Chen, J. (2020). A Modification in Coding and Non-coding RNAs: Roles and Therapeutic Implications in Cancer. Cancer Cell *37*, 270–288.
43. Deng, J., Zhang, J., Ye, Y., Liu, K., Zeng, L., Huang, J., Pan, L., Li, M., Bai, R., Zhuang, L., et al. (2021). N(6) -methyladenosine-Mediated Upregulation of WTAPP1 Promotes WTAP Translation and Wnt Signaling to Facilitate Pancreatic Cancer Progression. Cancer Res. *81*, 5268–5283.
44. He, X., Tan, L., Ni, J., and Shen, G. (2021). Expression pattern of m(6)A regulators is significantly correlated with malignancy and antitumor immune response of breast cancer. Cancer Gene Ther. *28*, 188–196.
45. Ji, L., Chen, S., Gu, L., and Zhang, X. (2020). Exploration of Potential Roles of m6A Regulators in Colorectal Cancer Prognosis. Front. Oncol. *10*, 768.
46. Zhu, Q., Wu, X., Ma, L., and Xue, H. (2022). Apoptosis-Associated Gene Expression Profiling Is One New Prognosis Risk Predictor of Human Rectal Cancer. Dis. Markers *2022*, 4596810.
47. Xu, J., Dai, S., Yuan, Y., Xiao, Q., and Ding, K. (2020). A Prognostic Model for Colon Cancer Patients Based on Eight Signature Autophagy Genes. Front. Cell Dev. Biol. *8*, 602174.
48. Chen, S., Wang, Y., Wang, B., Zhang, L., Su, Y., Xu, M., and Zhang, M. (2021). A signature based on 11 autophagy genes for prognosis prediction of colorectal cancer. PLoS One *16*, e0258741.
49. Yang, Y., Feng, M., Bai, L., Zhang, M., Zhou, K., Liao, W., Lei, W., Zhang, N., Huang, J., and Li, Q. (2021). The Effects of Autophagy-Related Genes and lncRNAs in Therapy and Prognosis of Colorectal Cancer. Front. Oncol. *11*, 582040.
50. Zhu, S., Wu, Q., Zhang, B., Wei, H., Li, B., Shi, W., Fang, M., Zhu, S., Wang, L., Lang Zhou, Y., and Dong, Y. (2020). Autophagy-related gene expression classification defines three molecular subtypes with distinct clinical and microenvironment cell infiltration characteristics in colon cancer. Int. Immunopharmacol. *87*, 106757.
51. Chen, L., Zhang, K., Sun, J., Tang, J., and Zhou, J. (2021). J. Development and Validation of an Autophagy-Stroma-Based Microenvironment Gene Signature for Risk Stratification in Colorectal Cancer. OncoTargets Ther. *14*, 3503–3515.
52. Du, Y., Lin, Y., Wang, B., Li, Y., Xu, D., Gan, L., Xiong, X., Hou, S., Chen, S., Shen, Z., and Ye, Y. (2022). Cuproptosis patterns and tumor immune infiltration characterization in colorectal cancer. Front. Genet. *13*, 976007.
53. Huang, H., Long, Z., Xie, Y., Qin, P., Kuang, L., Li, X., Zhao, Y., Zhang, X., Yang, L., Ma, W., et al. (2022). Molecular Subtypes Based on Cuproptosis-Related Genes and Tumor Microenvironment Infiltration Characterization in Colorectal Cancer. J. Oncol. *2022*, 5034092.
54. Xu, C., Liu, Y., Zhang, Y., and Gao, L. (2022). The role of a cuproptosis-related prognostic signature in colon cancer tumor microenvironment and immune responses. Front. Genet. *13*, 928105.
55. Liu, Y., Guo, F., Guo, W., Wang, Y., Song, W., and Fu, T. (2021). Ferroptosis-related genes are potential prognostic molecular markers for patients with colorectal cancer. Clin. Exp. Med. *21*, 467–477.
56. Du, S., Zeng, F., Sun, H., Liu, Y., Han, P., Zhang, B., Xue, W., Deng, G., Yin, M., and Cui, B. (2022). Prognostic and therapeutic significance of a novel ferroptosis related signature in colorectal cancer patients. Bioengineered *13*, 2498–2512.
57. Shao, Y., Jia, H., Huang, L., Li, S., Wang, C., Aikemu, B., Yang, G., Hong, H., Yang, X., Zhang, S., et al. (2021). An Original Ferroptosis-Related Gene Signature Effectively Predicts the Prognosis and Clinical Status for Colorectal Cancer Patients. Front. Oncol. *11*, 711776.
58. Liang, X., Cheng, Z., Chen, X., and Li, J. (2022). Prognosis analysis of necroptosis-related genes in colorectal cancer based on bioinformatic analysis. Front. Genet. *13*, 955424.
59. Peng, X., Xu, Z., Guo, Y., and Zhu, Y. (2022). Necroptosis-Related Genes Associated With Immune Activity and Prognosis of Colorectal Cancer. Front. Genet. *13*, 909245.
60. Zheng, C., and Tan, Z. (2021). A novel identified pyroptosis-related prognostic signature of colorectal cancer. Math. Biosci. Eng. *18*, 8783–8796.
61. Rao, J., Li, W., and Chen, C. (2021). Pyroptosis-Mediated Molecular Subtypes

and Tumor Microenvironment Infiltration Characterization in Colon Cancer. Front. Cell Dev. Biol. *9*, 766503.
62. Lu, H., Sun, Y., Zhu, Z., Yao, J., Xu, H., Huang, R., and Huang, B. (2022). Pyroptosis is related to immune infiltration and predictive for survival of colon adenocarcinoma patients. Sci. Rep. *12*, 9233.
63. Li, Z., Liu, Y., Lin, B., Yan, W., Yi, H., Wang, H., and Wei, Y. (2022). Pyroptosis-Related Signature as Potential Biomarkers for Predicting Prognosis and Therapy Response in Colorectal Cancer Patients. Front. Genet. *13*, 925338.
64. Wei, R., Li, S., Yu, G., Guan, X., Liu, H., Quan, J., Jiang, Z., and Wang, X. (2021). Deciphering the Pyroptosis-Related Prognostic Signature and Immune Cell Infiltration Characteristics of Colon Cancer. Front. Genet. *12*, 755384.
65. Zhuang, Z., Cai, H., Lin, H., Guan, B., Wu, Y., Zhang, Y., Liu, X., Zhuang, J., and Guan, G. (2021). Development and Validation of a Robust Pyroptosis-Related Signature for Predicting Prognosis and Immune Status in Patients with Colon Cancer. J. Oncol. *2021*, 5818512.
66. Yu, W., He, G., Zhang, W., Ye, Z., Zhong, Z., and Huang, S. (2022). INHBB is a novel prognostic biomarker and correlated with immune infiltrates in gastric cancer. Front. Genet. *13*, 933862.
67. Yuan, J., Xie, A., Cao, Q., Li, X., and Chen, J. (2020). INHBB Is a Novel Prognostic Biomarker Associated with Cancer-Promoting Pathways in Colorectal Cancer. BioMed Res. Int. *2020*, 6909672.
68. Dong, B., and Wu, Y. (2021). Epigenetic Regulation and Post-Translational Modifications of SNAI1 in Cancer Metastasis. Int. J. Mol. Sci. *22*, 11062.
69. Tang, X., Sui, X., Weng, L., and Liu, Y. (2021). SNAIL1: Linking Tumor Metastasis to Immune Evasion. Front. Immunol. *12*, 724200.
70. Galindo-Pumariño, C., Collado, M., Castillo, M.E., Barquín, J., Romio, E., Larriba, M.J., Muñoz de Mier, G.J., Carrato, A., de la Pinta, C., and Pena, C. (2022). SNAI1-expressing fibroblasts and derived-extracellular matrix as mediators of drug resistance in colorectal cancer patients. Toxicol. Appl. Pharmacol. *450*, 116171.
71. Shen, T., Yue, C., Wang, X., Wang, Z., Wu, Y., Zhao, C., Chang, P., Sun, X., and Wang, W. (2021). NFATc1 promotes epithelial-mesenchymal transition and facilitates colorectal cancer metastasis by targeting SNAI1. Exp. Cell Res. *408*, 112854.
72. Zhang, N., Ng, A.S., Cai, S., Li, Q., Yang, L., and Kerr, D. (2021). Novel therapeutic strategies: targeting epithelial-mesenchymal transition in colorectal cancer. Lancet Oncol. *22*, e358–e368.
73. Pellarin, I., Dall'Acqua, A., Gambelli, A., Pellizzari, I., D'Andrea, S., Sonego, M., Lorenzon, I., Schiappacassi, M., Belletti, B., and Baldassarre, G. (2020). Splicing factor proline- and glutamine-rich (SFPQ) protein regulates platinum response in ovarian cancer-modulating SRSF2 activity. Oncogene *39*, 4390–4403.
74. Mitobe, Y., Iino, K., Takayama, K.I., Ikeda, K., Suzuki, T., Aogi, K., Kawabata, H., Suzuki, Y., Horie-Inoue, K., and Inoue, S. (2020). PSF Promotes ER-Positive Breast Cancer Progression via Posttranscriptional Regulation of ESR1 and SCFD2. Cancer Res. *80*, 2230–2242.
75. Hu, Z., Dong, L., Li, S., Li, Z., Qiao, Y., Li, Y., Ding, J., Chen, Z., Wu, Y., Wang, Z., et al. (2020). Splicing Regulator p54(nrb)/Non-POU Domain-Containing Octamer-Binding Protein Enhances Carcinogenesis Through Oncogenic Isoform Switch of MYC Box-Dependent Interacting Protein 1 in Hepatocellular Carcinoma. Hepatology *72*, 548–568.
76. Klotz-Noack, K., Klinger, B., Rivera, M., Bublitz, N., Uhlitz, F., Riemer, P., Lüthen, M., Sell, T., Kasack, K., Gastl, B., et al. (2020). SFPQ Depletion Is Synthetically Lethal with BRAF(V600E) in Colorectal Cancer Cells. Cell Rep. *32*, 108184.
77. Wang, D.D., Sun, D.L., Yang, S.P., Song, J., Wu, M.Y., Niu, W.W., Song, M., and Zhang, X.L. (2022). Long noncoding RNA TNFRSF10A-AS1 promotes colorectal cancer through upregulation of HuR. World J. Gastroenterol. *28*, 2184–2200.
78. Palladino, G., Notarangelo, T., Pannone, G., Piscazzi, A., Lamacchia, O., Sisinni, L., Spagnoletti, G., Toti, P., Santoro, A., Storto, G., et al. (2016). TRAP1 regulates cell cycle and apoptosis in thyroid carcinoma cells. Endocr. Relat. Cancer *23*, 699–709.
79. Jin, H., Ying, X., Que, B., Wang, X., Chao, Y., Zhang, H., Yuan, Z., Qi, D., Lin, S., Min, W., et al. (2019). N(6)-methyladenosine modification of ITGA6 mRNA promotes the development and progression of bladder cancer. EBioMedicine *47*, 195–207.
80. Schedin, P., and Keely, P.J. (2011). Mammary gland ECM remodeling, stiffness, and mechanosignaling in normal development and tumor progression. Cold Spring Harb. Perspect. Biol. *3*, a003228.
81. Mao, X., Xu, J., Wang, W., Liang, C., Hua, J., Liu, J., Zhang, B., Meng, Q., Yu, X., and Shi, S. (2021). Crosstalk between cancer-associated fibroblasts and immune cells in the tumor microenvironment: new findings and future perspectives. Mol. Cancer *20*, 131.
82. Zou, Y., Zheng, S., Deng, X., Yang, A., Xie, X., Tang, H., and Xie, X. (2019). The Role of Circular RNA CDR1as/ciRS-7 in Regulating Tumor Microenvironment: A Pan-Cancer Analysis. Biomolecules *9*, 429.
83. Qian, B.Z., and Pollard, J.W. (2010). Macrophage diversity enhances tumor progression and metastasis. Cell *141*, 39–51.
84. Zheng, S., Zou, Y., Xie, X., Liang, J.Y., Yang, A., Yu, K., Wang, J., Tang, H., and Xie, X. (2020). Development and validation of a stromal immune phenotype classifier for predicting immune activity and prognosis in triple-negative breast cancer. Int. J. Cancer *147*, 542–553.
85. Li, Y., Tian, R., Liu, J., Li, J., Tan, H., Wu, Q., and Fu, X. (2022). Deciphering the immune landscape dominated by cancer-associated fibroblasts to investigate their potential in indicating prognosis and guiding therapeutic regimens in high grade serous ovarian carcinoma. Front. Immunol. *13*, 940801.
86. Eide, P.W., Bruun, J., Lothe, R.A., and Sveen, A. (2017). CMScaller: an R package for consensus molecular subtyping of colorectal cancer pre-clinical models. Sci. Rep. *7*, 16618.
87. Zhang, B., Wu, Q., Li, B., Wang, D., Wang, L., and Zhou, Y.L. (2020). A regulator-mediated methylation modification patterns and tumor microenvironment infiltration characterization in gastric cancer. Mol. Cancer *19*, 53.
88. Chong, W., Shang, L., Liu, J., Fang, Z., Du, F., Wu, H., Liu, Y., Wang, Z., Chen, Y., Jia, S., et al. (2021). m(6 A regulator-based methylation modification patterns characterized by distinct tumor microenvironment immune profiles in colon cancer. Theranostics *11*, 2201–2217.
89. Friedman, J., Hastie, T., and Tibshirani, R. (2010). Regularization Paths for Generalized Linear Models via Coordinate Descent. J. Stat. Softw. *33*, 1–22.
90. Hänzelmann, S., Castelo, R., and Guinney, J. (2013). gene set variation analysis for microarray and RNA-seq data. BMC Bioinf. *14*, 7.
91. Wu, T., Hu, E., Xu, S., Chen, M., Guo, P., Dai, Z., Feng, T., Zhou, L., Tang, W., Zhan, L., et al. (2021). clusterProfiler 4.0: A universal enrichment tool for interpreting omics data. Innovation *2*, 100141.
92. Subramanian, A., Tamayo, P., Mootha, V.K., Mukherjee, S., Ebert, B.L., Gillette, M.A., Paulovich, A., Pomeroy, S.L., Golub, T.R., Lander, E.S., and Mesirov, J.P. (2005). Gene set enrichment analysis: a knowledge-based approach for interpreting genome-wide expression profiles. Proc. Natl. Acad. Sci. USA *102*, 15545–15550.
93. Yoshihara, K., Shahmoradgoli, M., Martínez, E., Vegesna, R., Kim, H., Torres-Garcia, W., Treviño, V., Shen, H., Laird, P.W., Levine, D.A., et al. (2013). Inferring tumour purity and stromal and immune cell admixture from expression data. Nat. Commun. *4*, 2612.
94. Racle, J., and Gfeller, D. (2020). EPIC: A Tool to Estimate the Proportions of Different Cell Types from Bulk Gene Expression Data. Methods Mol. Biol. *2120*, 233–248.
95. Becht, E., Giraldo, N.A., Lacroix, L., Buttard, B., Elarouci, N., Petitprez, F., Selves, J., Laurent-Puig, P., Sautès-Fridman, C., Fridman, W.H., and de Reyniès, A. (2016). Estimating the population abundance of tissue-infiltrating immune and stromal cell populations using gene expression. Genome Biol. *17*, 218.
96. Aran, D., Hu, Z., and Butte, A.J. (2017). digitally portraying the tissue cellular heterogeneity landscape. Genome Biol. *18*, 220.
97. Fu, J., Li, K., Zhang, W., Wan, C., Zhang, J., Jiang, P., and Liu, X.S. (2020). Large-scale public data reuse to model immunotherapy response and resistance. Genome Med. *12*, 21.
98. Newman, A.M., Liu, C.L., Green, M.R., Gentles, A.J., Feng, W., Xu, Y., Hoang, C.D., Diehn, M., and Alizadeh, A.A. (2015). Robust enumeration of cell subsets from tissue expression profiles. Nat. Methods *12*, 453–457.
99. Finotello, F., Mayer, C., Plattner, C., Laschober, G., Rieder, D., Hackl, H., Krogsdam, A., Loncova, Z., Posch, W., Wilflingseder, D., et al. (2019). Molecular and pharmacological modulators of the tumor immune contexture revealed by deconvolution of RNA-seq data. Genome Med. *11*, 34.
100. Zeng, D., Ye, Z., Shen, R., Yu, G., Wu, J., Xiong, Y., Zhou, R., Qiu, W., Huang, N., Sun, L., et al. (2021). IOBR: Multi-Omics Immuno-Oncology Biological Research to Decode Tumor Microenvironment and Signatures. Front. Immunol. *12*, 687975.

101. Charoentong, P., Finotello, F., Angelova, M., Mayer, C., Efremova, M., Rieder, D., Hackl, H., and Trajanoski, Z. (2017). Pan-cancer Immunogenomic Analyses Reveal Genotype-Immunophenotype Relationships and Predictors of Response to Checkpoint Blockade. Cell Rep. *18*, 248–262.

102. Yang, C., Huang, X., Li, Y., Chen, J., Lv, Y., and Dai, S. (2021). Prognosis and personalized treatment prediction in TP53-mutant hepatocellular carcinoma: an in silico strategy towards precision oncology. Brief. Bioinform. *22*, bbaa164.

103. Geeleher, P., Cox, N., and Huang, R.S. (2014). pRRophetic: an R package for prediction of clinical chemotherapeutic response from tumor gene expression levels. PLoS One *9*, e107468.

104. Liu, Z., Xu, H., Weng, S., Ren, Y., and Han, X. (2022). Stemness Refines the Classification of Colorectal Cancer With Stratified Prognosis, Multi-Omics Landscape, Potential Mechanisms, and Treatment Options. Front. Immunol. *13*, 828330.

105. Kang, L., Chen, W., Petrick, N.A., and Gallas, B.D. (2015). Comparing two correlated C indices with right-censored survival outcome: a one-shot nonparametric approach. Stat. Med. *34*, 685–703.

STAR★METHODS

KEY RESOURCES TABLE

REAGENT or RESOURCE	SOURCE	IDENTIFIER
Deposited data		
TCGA-COADREAD/CRC	TCGA	https://portal.gdc.cancer.gov/
GSE17537	GEO	https://www.ncbi.nlm.nih.gov/geo/query/acc.cgi?acc=GSE17537
GSE32323	GEO	https://www.ncbi.nlm.nih.gov/geo/query/acc.cgi?acc=GSE32323
GSE38832	GEO	https://www.ncbi.nlm.nih.gov/geo/query/acc.cgi?acc=GSE38832
GSE39582	GEO	https://www.ncbi.nlm.nih.gov/geo/query/acc.cgi?acc=GSE39582
IMvigor210	N/A	http://researchpub.gene.com/IMvigor210CoreBiologies
CTRP	N/A	https://portals.broadinstitute.org/ctrp/
PRISM	N/A	https://depmap.org/portal/prism/
Software and algorithm		
R version 4.2.2	N/A	https://www.r-project.org/
TCGAbiolinks	Bioconductor	https://bioconductor.org/packages/TCGAbiolinks/
maftools	Bioconductor	https://bioconductor.org/packages/maftools/
limma	Bioconductor	https://bioconductor.org/packages/limma/
CMScaller	Github	https://github.com/Lothelab/CMScaller
IOBP	Github	https://github.com/IOBR/IOBR
Graphpad Prism	N/A	https://www.graphpad.com/
Oligonucleotides		
INHBB		
Forward Primer: GTGAAGCGGCACATCTTGAG	Sangon Biotech	N/A
Reverse Primer: GCGAAGCTGATGATTTCGGAAAC	Sangon Biotech	N/A
FTO		
Forward Primer: ACTTGGCTCCCTTATCTGACC	Sangon Biotech	N/A
Reverse Primer: TGTGCAGTGTGAGAAAGGCTT	Sangon Biotech	N/A
SNAI1		
Forward Primer: TCGGAAGCCTAACTACAGCGA	Sangon Biotech	N/A
Reverse Primer: AGATGAGCATTGGCAGCGAG	Sangon Biotech	N/A
GAPDH		
Forward Primer: AACGGATTTGGTCGTATTGG	Sangon Biotech	N/A
Reverse Primer: TTGATTTTGGAGGGATCTCG	Sangon Biotech	N/A

RESOURCE AVAILABILITY

Lead contact

Further information and requests for resources and reagents should be directed to and will be fulfilled by the lead contact, Chunlin Ou (ouchunlin@csu.edu.cn) and Yimin Li (yimin_li_0107@163.com).

Materials availability

This study did not generate new unique reagents.

Data and code availability

This paper analyzes existing publicly available data. Accession numbers are listed in the key resources table. The original code and any additional information required to reanalyze the data reported in this paper is available from the lead contact upon request.

EXPERIMENTAL MODEL AND SUBJECT DETAILS

Cell lines

The human CRC cell lines HT29, HCT8, $CACO_2$, SW620, and HCT116 were procured from the American Type Culture Collection (ATCC; http://www.atcc.org/) and sustained in RPMI 1640 medium (Biological Industries, Kibbutz Belt HaEmek, Israel) supplemented with 10% fetal bovine serum. All cells were cultured under standard conditions at 37°C in the presence of 5% CO_2.

Human tissue specimens

We recruited a cohort of 30 CRC patients who underwent curative resection at Xiangya Hospital of Central South University. None of the patients received any preoperative chemotherapy or radiotherapy.

METHOD DETAILS

Data retrieval and preprocessing

We obtained gene expression profiles and relevant clinical information for CRC from The Cancer Genome Atlas (TCGA) dataset and the Gene Expression Omnibus (GEO) (Table S1). Data preprocessing followed established procedures.[85] Patients with incomplete overall survival information or a survival time of less than one month were excluded. For TCGA-COADREAD/CRC, we utilized the R package "TCGAbiolinks" to access RNA sequencing data (TPM values), mutation profiles, copy number variation (CNV) data, and clinical data. We employed the "maftools" R package for visualizing somatic mutation data and GISTIC2.0 (Gene Pattern) to detect somatic copy number variations. CMS subtypes were determined using the "CMScaller" package.[29,86] We integrated the meta-GEO dataset, which comprised 749 samples, including data from GSE17537 (54 samples), GSE38832 (122 samples), and GSE39582 (573 samples). Prior to merging different datasets in the meta-GEO dataset, batch effects were corrected. Additionally, we obtained data from the IMvigor210 cohort from the internet database.

Screening for m6A-associated PCD genes

We conducted a comprehensive review of the literature on m6A methylation modification and PCD patterns. This led to the curation and analysis of 23 m6A RNA methylation regulators and 1078 PCD-related genes.[8,87,88] Spearman correlation analysis was employed to assess the expression of PCD-related genes and m6A regulators. We filtered m6A-associated PCD-related genes under the conditions of |correlation coefficient (R)| $\geq$ 0.3 and P value $<$ 0.05.

Construction of the risk score model

Differentially expressed m6A-associated PCD genes between normal and CRC samples were identified using the empirical Bayesian approach from the "limma" R package, with significance criteria set at an adjusted P value $<$ 0.05 and $|\log_2 FC| \geq 0.5$. Subsequently, univariate Cox regression analysis and Kaplan-Meier survival analysis were performed on the identified genes to identify prognostic m6A-associated PCD genes. To minimize omissions, we adjusted the cut-off P value in Cox analysis to 0.1 and P value in Log-rank tests to 0.01. The LASSO Cox regression algorithm was further applied to reduce the number of candidate m6A-associated PCD genes and construct the most suitable signature.[89] The cell death-related risk score (CDRS) model was established using the following formula:

$$\mathrm{CDRS} = \sum_{i=1}^{10} \beta i * Ei$$

βi denote the risk coefficient and Ei refer to the expression of each gene. The CRC patients were divided into high- or low-CDRS groups based on the median value. Additionally, we employed the receiver operating characteristic (ROC) curve, area under the curve (AUC), and concordance (c)-index to assess the prediction accuracy of the CDRS model. Furthermore, we developed a prognostic nomogram for CRC patients based on clinical features and CDRS. The efficacy of the nomogram was evaluated using calibration plots and decision curve analysis (DCA).

Functional enrichment analysis

To explore potential differences in biological processes between the high- and low-CDRS groups, we conducted GSVA enrichment analysis using the "GSVA" R package.[90] We also performed gene set enrichment analysis (GSEA) using the "clusterProfiler" R package.[91] The gene sets "h.all.v7.5.1.symbols" and "c2.cp.kegg.v7.5.1.symbols" were downloaded from the MSigDB database (https://www.gsea-msigdb.org/gsea/msigdb/index.jsp).[92]

Tumor microenvironment analysis

The immunological score, stromal score, ESTIMATE score, and tumor purity were determined using the "ESTIMATE" program.[93] To quantify the relative abundance of each cell infiltration in CRC, we employed the EPIC algorithm.[94] Additionally, we utilized six independent algorithms: EPIC, MCP-COUNTER, XCELL, TIDE, CIBERSORT, and QUANTISEQ to calculate the infiltration level of cancer-associated fibroblasts (CAFs), epithelial cells, and macrophages.[94–99] The cancer-related signatures were obtained and evaluated using the "IOBP" package.[100] We

employed the Tumor Immune Dysfunction and Exclusion (TIDE) and Immunophenoscore (IPS) algorithms to predict the response to immunotherapy in different CRC subtypes.[97,101]

RNA extraction and real-time quantitative PCR (qPCR)

Total RNA was extracted from cells using FFPE RNA Extraction Kits (AmoyDx, Xiamen, China) in accordance with the manufacturer's instructions. The quality and concentration of RNA were evaluated using the NanoDrop 1000 Spectrophotometer (Thermo Fisher, USA), with OD260/OD280 ratios ranging from 1.8 to 2.0 and OD260/230 ratios from 2.0 to 2.2 deemed acceptable. The first-strand cDNA was synthesized from 1 μg of total RNA using HiScript II Reverse Transcriptase (Vazyme, Nanjing, China). Quantitative real-time PCR (qPCR) was conducted on an ABI Prism 700 thermal cycler (Applied Biosystems, Foster City, CA, USA). Relative RNA quantification was normalized to GAPDH expression, and all experiments were performed in triplicate.

Potential therapeutic agents

We retrieved the drug sensitivity data for cancer cell lines from two sources: the Cancer Therapeutics Response Portal (CTRP, https://portals.broadinstitute.org/ctrp/) and the Profiling Relative Inhibition Simultaneously in Mixtures dataset (PRISM https://depmap.org/portal/prism/).[102] We excluded compounds with missing values greater than 20% and used K-nearest neighbor (k-NN) imputation to fill in the missing AUC values. To predict drug response in clinical samples, we employed the built-in ridge regression model from the pRRophetic package.[103,104] The predicted AUC values were used to assess drug sensitivity, where lower AUC values indicated increased sensitivity to treatment.[102] Finally, we performed differential drug response analysis and Spearman correlation analysis to identify potential therapeutic agents.

Statistical analysis

All bioinformatics analyses were performed using R and Graphpad Prism (presented as mean +/- SD). Student's t-test and one-way ANOVA were conducted to compare differences between two or multiple normally distributed groups, respectively. The Wilcoxon test or Kruskal-Wallis test was used for non-normally distributed data to compare differences between two groups or among multiple groups, respectively. Correlations between continuous variables were analyzed using Spearman's correlation analysis. Differences between categorical variables were evaluated using chi-square and Fisher's exact tests. ROC curves were generated using the "pROC" R package, and the C-indices of different variables were compared using the "CompareC" package.[105] Survival curves were described by Kaplan-Meier plots and compared with the log-rank test. Univariate Cox regression analysis was performed to estimate hazard ratios (HR) for CDRS and m6A-associated PCD genes. Independent prognostic factors were determined using multivariable Cox regression analysis. A two-sided P value < 0.05 was considered statistically significant for all analyses.